Journal of Organometallic Chemistry 902 (2019) 120955

Contents lists available at ScienceDirect

Journal of Organometallic Chemistry

journal homepage: www.elsevier.com/locate/jorganchem

Synthesis of P(FHEMA-*co*-MAZO-*co*-MAA)s copolymers and their redox and photo-responsive properties

Amin Khan [a], Haojie Yu [a, **], Yang Wang [b], Li Wang [a, *], Raja Summe Ullah [a], Fazal Haq [a], Tarig Elshaarani [a], Muhammad Usman [a], Ahsan Nazir [a], Kaleem-ur-Rehman Naveed [a]

[a] State Key Laboratory of Chemical Engineering, College of Chemical and Biological Engineering, Zhejiang University, Hangzhou, 310027, PR China
[b] Hangzhou Talent Research Institute, Hangzhou, 310000, PR China

ARTICLE INFO

Article history:
Received 4 May 2019
Received in revised form
17 September 2019
Accepted 25 September 2019
Available online 27 September 2019

Keywords:
Ferrocene
Azobenzene
Information storage
Methacrylic acid

ABSTRACT

Different copolymers (poly(2-(methacryloyloxy) ethyl ferrocene carboxylate-*co*-methacrylo-4-aminoazobenzene-*co*-methacrylic acid)s) (P(FHEMA-*co*-MAZO-*co*-MAA)s) were synthesized and their different properties were analyzed in this work. Methacrylic acid was introduced as a side group to possibly affect the photostability. The synthesized copolymers were characterized by nuclear magnetic resonance (^{1}H NMR) spectroscopy and gel permeation chromatography (GPC). Thermal studies were performed by thermogravimetric (TG), differential thermogravimetric (DTG) and differential scanning calorimetry (DSC) analysis, which showed that the copolymers were thermally stable under the operating conditions of the information storage devices. Redox studies and photoresponsive studies were performed by CV technique and UV/vis spectroscopy which showed that these copolymers contained good redox and photoresponsive properties. The obtained results paved the way towards the four states information storage of the materials.

1. Introduction

The booming demand for information data is promoting the approach towards the fabrication of innovative information storage materials. Such materials are categorized based on fast speed and response, low processing cost, easy processing, and high storage density [1,2]. Recently, significant attention has been gained by polymeric materials because of their outstanding features comprising 3-D stacking capability, structural simplicity, solution processability, mechanical features and so on [3,4]. The polymeric memory materials usually contain different sets of groups such as redox and photo responsive, vinyl-based particular pendant groups and so on. Out of these materials, redox and the photo responsive system showed high chemical and thermal stability, extraordinary resistance to harsh environments and commendable mechanical properties. Therefore this system is supposed to be the most appropriate candidates for information storage materials [5–8]. Among several different redox-responsive systems, ferrocene has attained utmost research interest because of its ultimate features such as high chemical and thermal stability, better solubility and good electrochemical property [9–11], ever since the first ferrocene-based system was reported [12]. As a result of the stable redox-activity of ferrocene, it can be used in different polymeric structures [13–16]. Ferrocene (Fe^{2+}) and its oxidized form ferrocenium (Fe^{3+}) can be reversibly switched between two stable states, consequently providing the opportunity for data storage [17]. Li and co-workers prepared a self-assembled monolayer of 4-ferrocenylbenzyl alcohol attached to silicon providing the root for electrolyte-molecule-silicon materials. The reversible charge trapping by these molecules recommended their potential application in memory devices [18]. In another work, the same group investigated few mixed self-assembled monolayers of redox active molecules (ferrocene) on Si which showed multiple definite redox states. The results indicated that these materials can be used for the redox responsive information storage [19]. Conversely, the scientific community also showed great attention to photoresponsive chromophores such as azobenzenes due to their ability to go through chemical, mechanical or optical change when exposed to specific light wavelength. A lot of possible applications such as information storage, liquid crystal displays, optical switching, surface relief gratings, molecular machines, nanodevices, and

* Corresponding author.
** Corresponding author.
E-mail addresses: hjyu@zju.edu.cn (H. Yu), opl_wl@dial.zju.edu.cn (L. Wang).

https://doi.org/10.1016/j.jorganchem.2019.120955
0022-328X/

nonlinear optics can be found by means of these azobenzene-based systems [20–25]. Azobenzene can switch its states very efficiently between *trans* (a planar state) and *cis* (a twisted state) in response to the specific wavelengths of light or thermal environment such as heat [26–29]. Azobenzene chromophore changes its mechanical properties in a polymer matrix by 39% owing to the distance between the two benzene rings, which becomes 5.5 Å from 9 Å after the light irradiation [30,31]. Lim and co-workers fabricated a storage device by using azobenzene chromophore in the donor-acceptor system. The results showed that the reversibility or rewritability of the storage media was reliant on the terminal moiety of the azobenzene chromophore [32]. Zhang and co-workers designed a novel azobenzene and graphene oxide based storage material which was functionalized with poly(*N*-vinylcarbazole). This effort provided a unique design methodology for ternary memory materials that could prominently improve the storage capacity of polymer memory devices [33]. Though, all these systems (redox/photo) existed simply on the basis of the two states (oxidation/reduction or *trans*/*cis*). At this time, it is required to move our methodologies to the four states information storage by the combined influence of ferrocene and azobenzene (redox and light). In our recent work, we developed an idea concerning the four states information storage by decreasing the photo-oxidation and π-π stacking of the azobenzene chromophore [34]. In this work, we have shifted our focus towards the photostability of azobenzene chromophore which is also a vital parameter to consider for storage devices [35]. In this respect, we will include methacrylic acid as a third monomer which possibly affects and improves the properties of the copolymers [35]. For this purpose, poly(2-meth acryloyloxy ethyl ferrocene carboxylate-*co*-meth-acrylo-4-amino azobenzene-*co*-meth acrylic acids)s (P(FHEMA-*co*-MAZO-*co*-MAA)s) will be synthesized and their reversible redox and photoresponsive properties will be investigated.

2. Experimental section

2.1. Materials

Dichloromethane (DCM, analytical reagent (AR)), tetrahydrofuran (THF, AR), triethylamine (Et_3N, AR) and pyridine (AR) were supplied by Sinopharm Chemical Reagent Co. Ltd. Methacrolyl chloride (95%), methacrylic acid (MAA) and hydroxyethyl methacrylate (HEMA, 96%) were purchased from Acros Organics. Azobisisobutyronitrile (AIBN) and ferrocene carboxylic acid (AR) were supplied by Aladdin. 4-Aminoazobenzene and tetrabutylammonium tetrafluoroborate (Bu_4NBF_4) were purchased from J & K Scientific Co. Ltd. DCM and Et_3N were dried firstly by activated 4 Å-type molecular sieves and then distilled over calcium hydride while THF was dried firstly by activated 4 Å-type molecular sieves and then distilled over potassium. Pyridine was also dried using activated 4 Å-type molecular sieves. Other chemicals were used without further purification.

2.2. Synthesis of 2-(methacryloyloxy)ethyl ferrocene carboxylate (FHEMA)

Ferrocene carbonyl chloride was synthesized according to the reported literature [36]. Firstly, ferrocene monocarbonyl chloride (6.3112 g, 24.4 mmol) was dissolved in 60.0 mL of THF and then pyridine (1.9 mL, 24.6 mmol) and HEMA (3.1 mL, 24.7 mmol) were added to the previous solution under inert (Ar gas) atmosphere. The reaction was refluxed for 5 h and after that the precipitates were separated from the reaction media by filtration. The obtained filtrate was dried by using rotary evaporator. Finally, the washing was performed using Na_2CO_3 (saturated solution) and deionized water twice (each one) to convert the crude product obtained from rotary evaporation to pure product. The pure product (FHEMA) was retained in a vacuum oven at 40 °C until the complete removal of residual solvents.

2.3. Synthesis of methacrylo-4-aminoazobenzene (MAZO)

Firstly, AZO (4.6001 g, 20.2 mmol) was dissolved in DCM (80.0 mL) under an inert atmosphere. After that, TEA (3.0 mL, 21.5 mmol) was added in the previous solution. Methacrolyl chloride (2.9 mL, 30.3 mmol) was added dropwise at 0 °C in the same solution and then the reaction was proceeded at this stage for 2 h and for 8 h at room temperature. Afterward, the precipitates were separated from the reaction media by filtration. The obtained filtrate was dried by using rotary evaporator. Finally, the washing was accomplished using Na_2CO_3 (saturated solution) and deionized water twice (each one) to convert the crude product obtained from rotary evaporation to pure product. The pure product (MAZO) was placed in a vacuum oven at 40 °C until the complete removal of residual solvents.

2.4. Synthesis of poly(methacrylo-4-aminoazobenzene) (PMAZO)

In a typical synthesis, MAZO (0.2652 g, 1.0 mmol) and AIBN (1.6 mg, 0.01 mmol) were dissolved in DMF (1.5 mL). The flask was purged with Ar gas first for 0.5 h to eradicate the availability of oxygen. After that, the reaction mixture was stirred for 12 h at 90 °C. After completing the reaction, the reaction mixture was added dropwise in methanol (250 mL) to get the precipitates. The precipitates were further purified by repeated dissolution in THF and precipitation in methanol twice. Finally, the resulting solution was centrifuged, filtered and the obtained solid after filtration was placed in a vacuum oven for the removal of residual solvents to get PMAZO.

2.5. Synthesis of poly(2-(methacryloyloxy) ethyl ferrocene carboxylate) (PFHEMA)

In a typical synthesis, FHEMA (0.3429 g, 1.0 mmol) and AIBN (1.6 mg, 0.01 mmol) were dissolved in DMF (1.5 mL). The flask was purged with Ar gas first for 15 min to eradicate the availability of oxygen. After that, the reaction mixture was stirred for 12 h at 90 °C. After completing the reaction, the reactions mixture was added dropwise in methanol (250 mL) to get the precipitates. The precipitates were further purified by repeated dissolution in THF and precipitation in methanol twice. Finally, the resulting solution was centrifuged, filtered and the obtained solid after filtration was placed in a vacuum oven for the removal of residual solvents to get PFHEMA.

2.6. Synthesis of poly(2-(methacryloyloxy) ethyl ferrocene carboxylate-co-(methacrylo-4-aminoazobenzene)) P(FHEMA-co-MAZO)

For the typical copolymerization of FHEMA and MAZO, free radical polymerization technique was adapted [37]. In the typical synthesis, FHEMA (0.3420 g, 1.0 mmol), MAZO (0.2652 g, 1.0 mmol) and AIBN (0.0033 g, 0.02 mmol) were dissolved in DMF (1.5 mL). The flask was purged with Ar gas first for 0.5 h to eradicate the availability of oxygen. After that, the reaction mixture was stirred for 12 h at 90 °C. After completing the reaction, the reaction mixture was added dropwise in methanol (250 mL) to get the precipitates. The precipitates were further purified by repeated dissolution in THF and precipitation in methanol twice. Finally, the resulting solution was centrifuged, filtered and the obtained solid

after filtration was placed in a vacuum oven for the removal of residual solvents to get the product.

2.7. Synthesis of poly(2-(methacryloyloxy) ethyl ferrocene carboxylate-co-(methacrylic acid)) P(FHEMA-co-MAA)

For the typical copolymerization of FHEMA and MAA, FHEMA (0.3420 g, 1.0 mmol), MAA (85 μL, 1.0 mmol) and AIBN (0.0037 g, 0.02 mmol) were dissolved in DMF (1.5 mL). The flask was purged with Ar gas first for 0.5 h to eradicate the availability of oxygen. After that, the reaction was carried out for 12 h at 90 °C. After completing the reaction, the reaction mixture was added dropwise in methanol (250 mL) to get the precipitates. The precipitates were further purified by repeated dissolution in THF and precipitation in methanol twice. Finally, the resulting solution was centrifuged, filtered and the obtained solid after filtration was placed in a

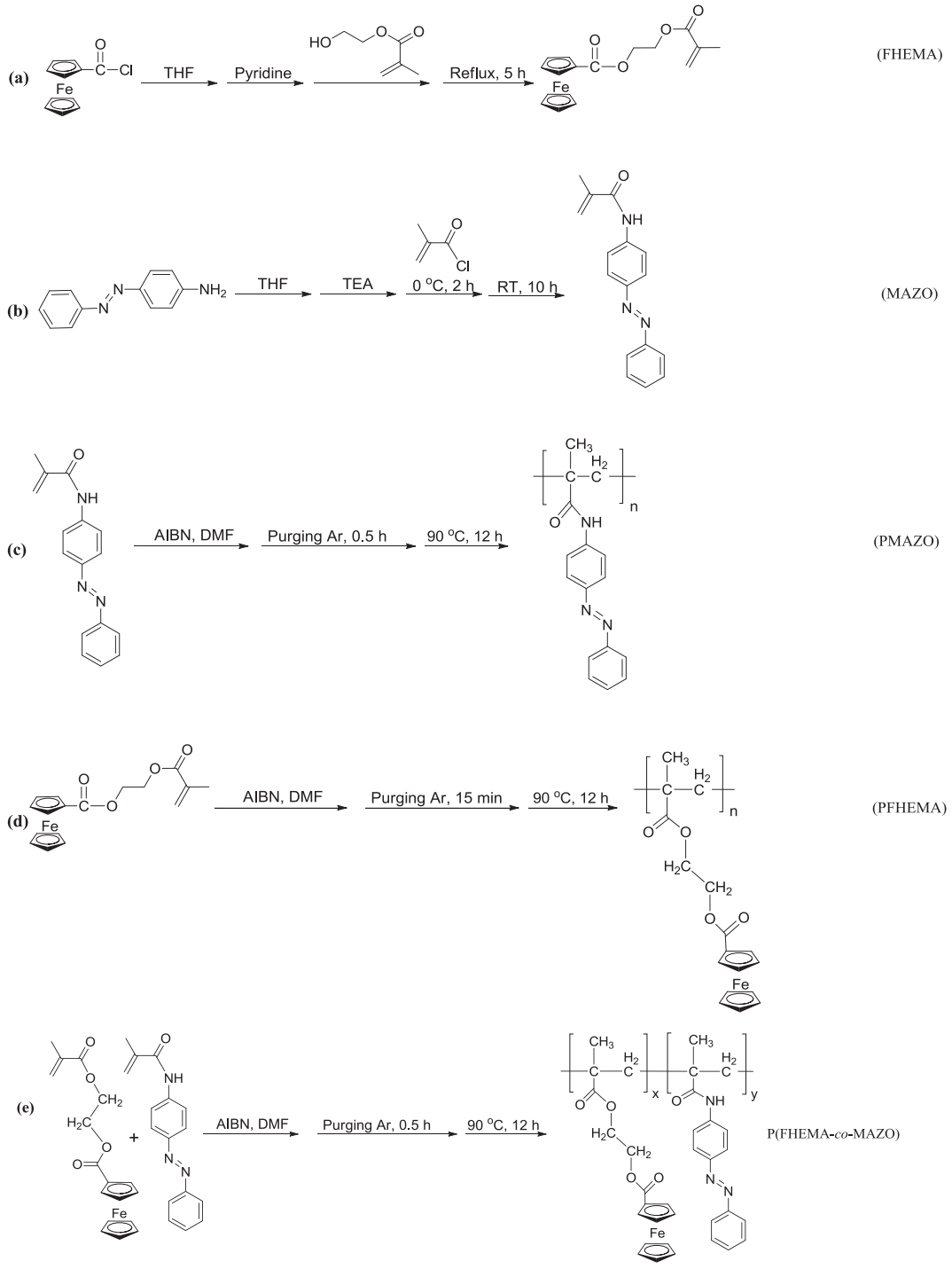

Scheme 1. Synthetic reactions for (a) FHEMA, (b) MAZO, (c) PMAZO, (d) PFHEMA, (e) P(FHEMA-*co*-MAZO), (f) P(FHEMA-*co*-MAA), (g) P(MAZO-*co*-MAA) and (h) P(FHEMA-*co*-MAZO-*co*-MAA).

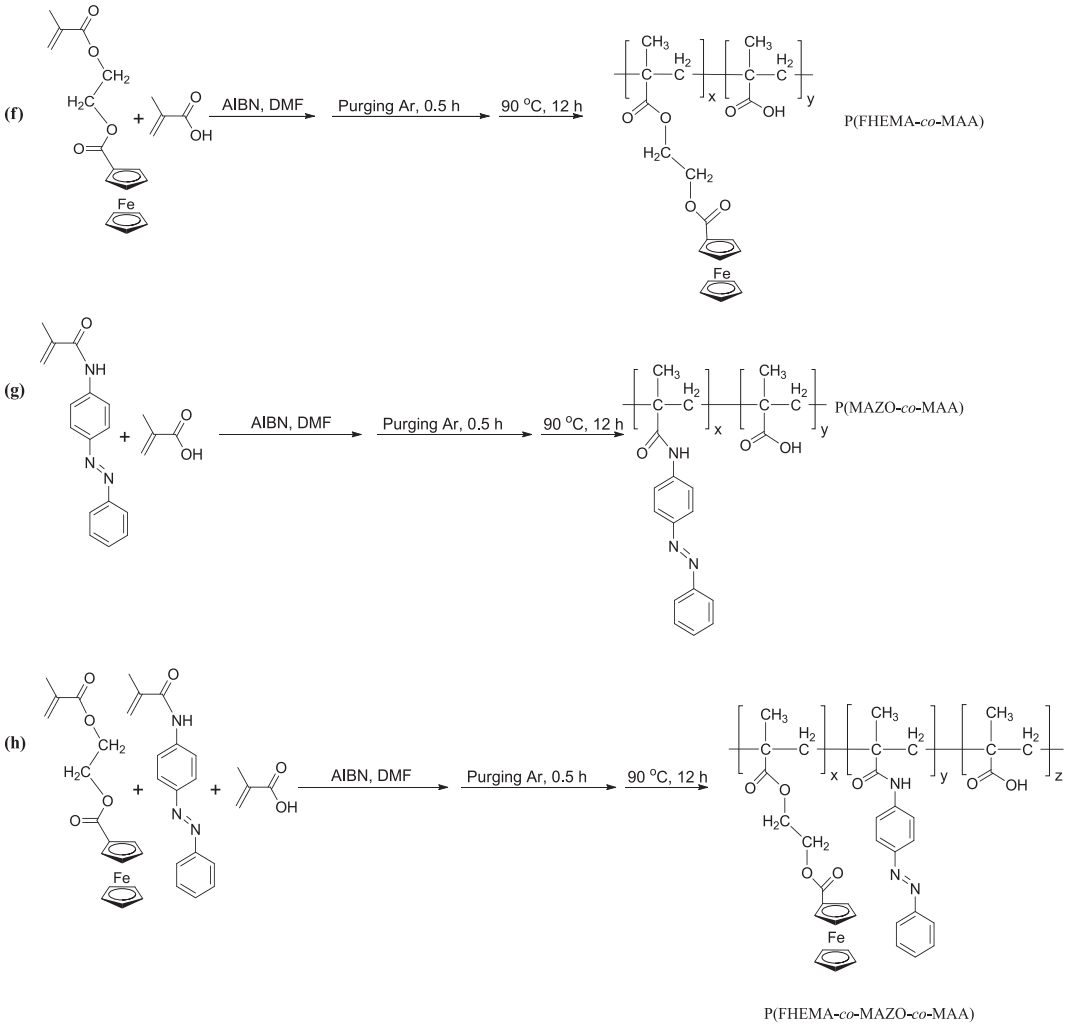

Scheme 1. (*continued*).

vacuum oven for the removal of residual solvents to get the product.

2.8. Synthesis of poly(methacrylo-4-amino azobenzene-co-(methacrylicacid)) P(MAZO-co-MAA)

For the typical copolymerization of MAZO and MAA, MAZO (0.2652 g, 1.0 mmol), MAA (85 μL, 1.0 mmol) and AIBN (0.0038 g, 0.02 mmol) were dissolved in DMF (1.5 mL). The flask was purged with Ar gas first for 0.5 h to eradicate the availability of oxygen. After that, the reaction was carried out for 12 h at 90 °C. After completing the reaction, the reaction mixture was added dropwise in methanol (250 mL) to get the precipitates. The precipitates were further purified by repeated dissolution in THF and precipitation in methanol twice. Finally, the resulting solution was centrifuged, filtered and the obtained solid after filtration was placed in a vacuum oven for the removal of residual solvents to get the product.

2.9. Synthesis of poly(2-(methacryloyloxy) ethyl ferrocene carboxylate-co-methacrylo-4-aminoazobenzene-co-methacrylic acid) P(FHEMA-co-MAZO-co-MAA)

For the typical copolymerization of FHEMA, MAZO and MAA, free radical polymerization technique was carried out [37]. The synthetic procedure for all the obtained polymers is the same with the difference in the mole ratios of monomers (FHEMA, MAZO, MAA). Therefore, the synthesis of P(FHEMA-*co*-MAZO-*co*-MAA)-1 was taken as an example. In the typical synthesis, FHEMA (0.3420 g, 1.0 mmol), MAZO (0.2652 g, 1.0 mmol), MAA (85 μL, 1.0 mmol) and AIBN (0.0049 g, 0.03 mmol) were dissolved in DMF (2.0 mL). The flask was purged with Ar gas first for 0.5 h to eradicate the availability of oxygen. After that, the reaction was carried out for 12 h at 90 °C. After completing the reaction, the reaction mixture was added dropwise in methanol (250 mL) to get the precipitates. The precipitates were further purified by repeated dissolution in THF and precipitation in methanol twice. Finally, the resulting solution was centrifuged, filtered and the obtained solid after filtration was placed in a vacuum oven for the removal of residual solvents to get the product.

2.10. Characterization

^{1}H NMR spectra of the synthesized copolymers were recorded using a Bruker Advanx-600 MHz NMR spectrometer. The weight average molecular mass (M_w) and number average molecular mass (M_n) were determined with waters 1524/2414 as gel permeation chromatography (GPC) instrument. THF was used as a mobile phase and the molecular weight of all the copolymers was calibrated against polymethylmethacrylate (PMMA) standard. Fourier transform infrared (FT-IR) spectra were recorded using the KBr pellet

technique on a Jasco IR-700 infrared spectrophotometer in the range of 400–4000 cm^{-1}. Thermal stability and degradation of the polymers were measured using TA-Q500 (Metler-Toledo) with a heating rate of 10 °C/min. The glass transition temperature (T_g) of the polymers were obtained using DSC-Q200 with a heating rate of 10 °C/min. The photoisomerization behavior of the polymers was recorded using a UV/vis Unico spectrophotometer. The sample solution had a concentration of 0.05 mM for the analysis. The CV curves were recorded on a CHI-630A electro-chemical analyzer (CH Instruments, Inc., Austin, Texas). The concentration of polymers and electrolyte (Bu_4NBF_4) were 0.5 mM and 0.1 M respectively for all the samples. A silver (Ag) electrode was used as a reference electrode while a platinum wire electrode was used as the counter electrode. The working electrode (glassy carbon) was provided with a mirror finish using 0.05 μm Al_2O_3 paste followed by washing under ultrasonication with alcohol/deionized water for 30 s and finally dried at room temperature before use.

3. Results and discussion

3.1. Synthesis and characterization of P(FHEMA-co-MAZO-co-MAA)s

FHEMA was obtained by esterification reaction of ferrocene carbonyl chloride and HEMA (Scheme 1a). The synthesis of MAZO was successfully performed by amidation reaction of AZO and methacrolyl chloride (Scheme 1b). Free radical polymerization was executed to synthesize PMAZO, PFHEMA, P(FHEMA-*co*-MAZO), P(MAZO-*co*-MAA), P(FHEMA-*co*-MAA) and P(FHEMA-*co*-MAZO-*co*-MAA)s using AIBN as an initiator. The synthetic routes of PMAZO, PFHEMA, P(FHEMA-*co*-MAZO), P(FHEMA-*co*-MAA), P(MAZO-*co*-MAA) and P(FHEMA-*co*-MAZO-*co*-MAA) have been given in Scheme 1(c-h) respectively. The stepwise procedure for the synthesis of P(FHEMA-*co*-MAZO-*co*-MAA) has been given in Scheme 2.

Table 1 explains the synthetic details of the copolymers P(FHEMA-*co*-MAZO-*co*-MAA)s while Table 2 illustrates the obtained mole ratios and molecular weights of the copolymers. The structures of FHEMA, MAZO, PMAZO, PFHEMA, P(FHEMA-*co*-MAZO), P(FHEMA-*co*-MAA) and P(MAZO-*co*-MAA) respectively were confirmed by ^{1}H NMR as shown in Fig. 1(a–g) respectively.

The data of chemical shifts for FHEMA was as follows: δ (ppm) = 6.16 (1H, H_a), 5.61 (1H, H_b), 4.81 (2H, H_c), 4.45 (4H, H_d, H_e), 4.40 (2H, H_f), 4.19 (5H, H_g), 1.97 (3H, H_h).

Following chemical shifts were obtained in a result for MAZO: δ (ppm) = 7.44–7.95 (9H, H_a-H_e), 5.83 (1H, H_f), 5.51 (1H, H_g), 2.09 (3H, H_h).

The characteristic peak shifts for PMAZO were as follows: δ (ppm) = 9.40 (H_a), 7.32–7.83 (H_b-H_f), 1.94–2.31 (H_g), 1.00–1.37 (H_h).

The characteristic peak shifts for PFHEMA were as follows: δ (ppm) = 4.76 (H_a), 4.27–4.52 (H_b, H_d, H_e), 4.19 (H_c), 1.66–2.01 (H_f), 0.84–1.15 (H_g).

The chemical shifts for P(FHEMA-*co*-MAZO) were as follows: δ (ppm) = 9.46 (H_a), 7.35–7.90 (H_b-H_f), 4.70 (H_g), 4.19–4.44 (H_h, H_i, H_j), 4.09 (H_k), 1.56–2.08 (H_l, H_m), 0.78–1.29 (H_n, H_o).

The chemical shifts for P(FHEMA-*co*-MAA) were as follows: δ (ppm) = 12.44 (H_a), 4.76 (H_b), 4.26–4.49 (H_c, H_d, H_e), 4.20 (H_f), 1.63–1.98 (H_g, H_h), 0.83–1.14 (H_i, H_j).

The chemical shifts for P(MAZO-*co*-MAA) were as follows: δ (ppm) = 12.27 (H_a), 9.47 (H_b), 7.37–7.90 (H_c-H_g), 1.46–1.95 (H_h, H_i), 0.82–1.16 (H_j, H_k).

^{1}H NMR spectra (Fig. 1) showed that the signals of azobenzene appear between 7.25 and 8.0 ppm while the signals of ferrocene appear in the region of 4.0–5.0 ppm. Different copolymers were synthesized by using different mole ratios of the monomers (Table 1). Fig. 2 represents the comparison of ^{1}H NMR spectra of P(FHEMA-*co*-MAZO-*co*-MAA)s copolymers.

From the ^{1}H NMR spectra, it is quite evident that the copolymers carried no unreacted monomers as the signals of the double bond which usually exist between 5.5 and 6.5 ppm have completely vanished. The copolymers were also characterized using FT-IR

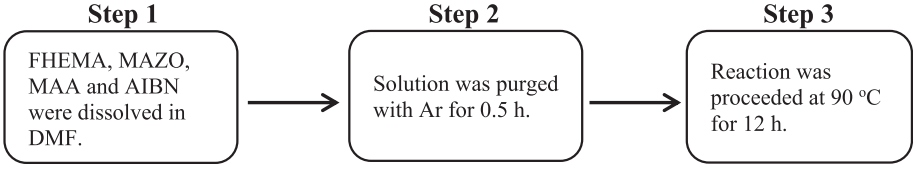

Scheme 2. Stepwise procedure for the synthesis of P(FHEMA-*co*-MAZO-*co*-MAA).

Table 1
Synthetic details of P(FHEMA-*co*-MAZO-*co*-MAA)s.

Sample	Step 1										Step 2	Step 3	
	FHEMA (A)		MAZO (B)		MAA (C)		AIBN (D)		Mole ratio	DMF	Ar purging	T	t
	g	mmol	g	mmol	μL	mmol	g	mmol	A:B:C:D	mL	h	°C	h
P(FHEMA-*co*-MAZO-*co*-MAA)-1	0.3420	1.00	0.2652	1.00	85	1.00	0.0049	0.03	1:1:1:0.03	2	0.5	90	12
P(FHEMA-*co*-MAZO-*co*-MAA)-2	0.6860	2.00	0.2660	1.01	85	1.00	0.0065	0.04	2:1:1:0.04	2	0.5	90	12
P(FHEMA-*co*-MAZO-*co*-MAA)-3	1.0290	3.00	0.2655	1.00	85	1.00	0.0082	0.05	3:1:1:0.05	2	0.5	90	12

Table 2
GPC results and ratios of each unit.

Sample	P(FHEMA-*co*-MAZO-*co*-MAA)s (GPC)			P(FHEMA-*co*-MAZO-*co*-MAA)s (NMR, GPC)			
	Mn	Mw	PDI	(x:y:z) (NMR)	m(FHEMA)	n(MAZO)	o(MAA)
P(FHEMA-*co*-MAZO-*co*-MAA)-1	7.6×10^3	1.1×10^4	1.49	0.98:1:0.96	3.6	3.7	3.6
P(FHEMA-*co*-MAZO-*co*-MAA)-2	6.0×10^3	8.6×10^3	1.41	1.98:1:0.92	4.4	2.2	2.1
P(FHEMA-*co*-MAZO-*co*-MAA)-3	4.9×10^3	9.3×10^3	1.90	2.96:1:0.89	4.3	1.5	1.3

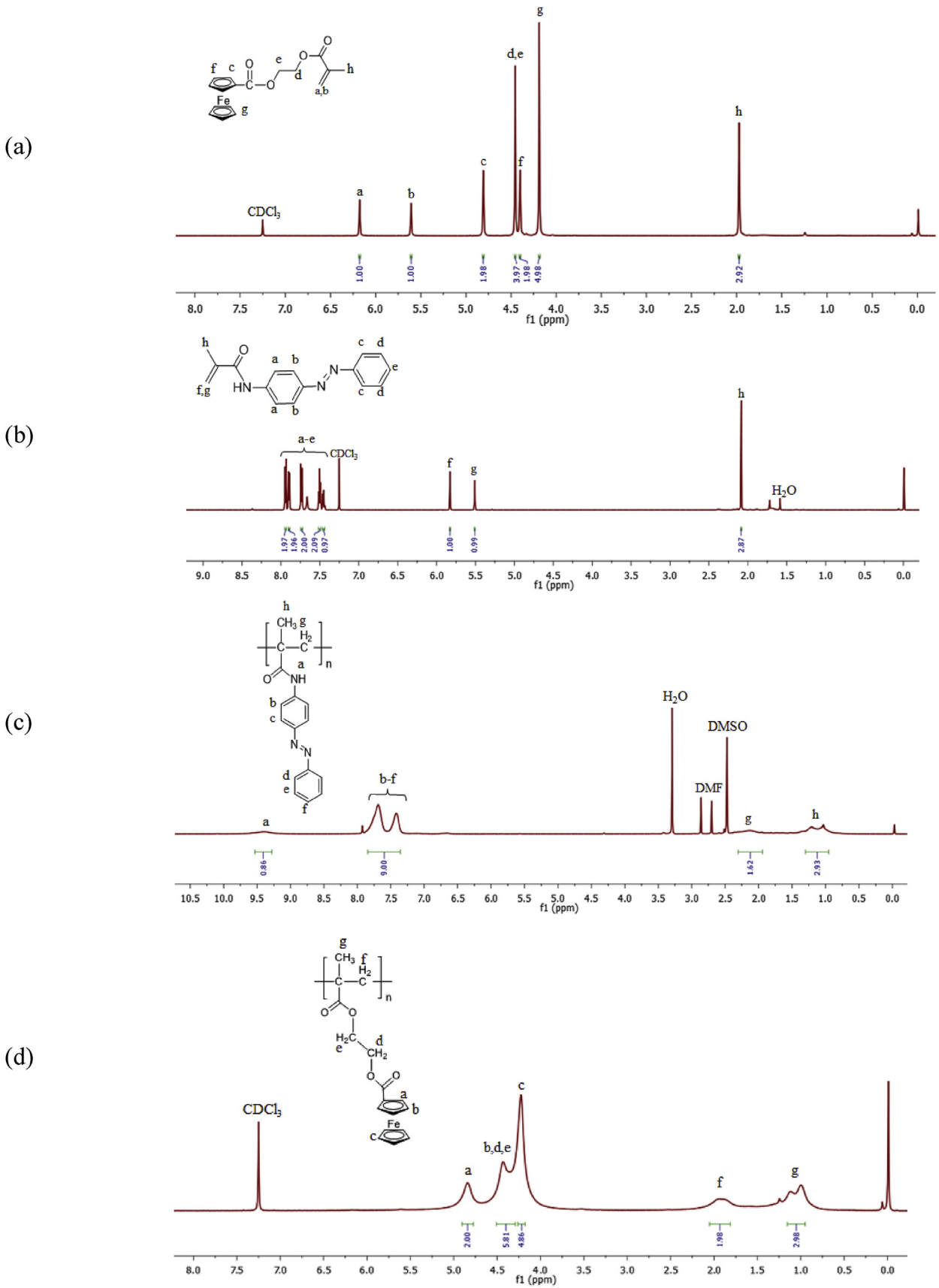

Fig. 1. [1]H NMR spectra of (a) FHEMA, (b) MAZO, (c) PMAZO, (d) PFHEMA, (e) P(FHEMA-*co*-MAZO), (f) P(FHEMA-*co*-MAA) and (g) P(MAZO-*co*-MAA). The chemical shifts for P(FHEMA-*co*-MAZO-*co*-MAA)-3 were as follows: δ (ppm) = 12.36 (H_a), 7.40–7.91 (H_b-H_f), 4.73 (H_g), 4.22–4.45 (H_h, H_i, H_j), 4.16 (H_k), 1.65–2.09 (H_l, H_m, H_n), 0.86–1.11 (H_o, H_p, H_q).

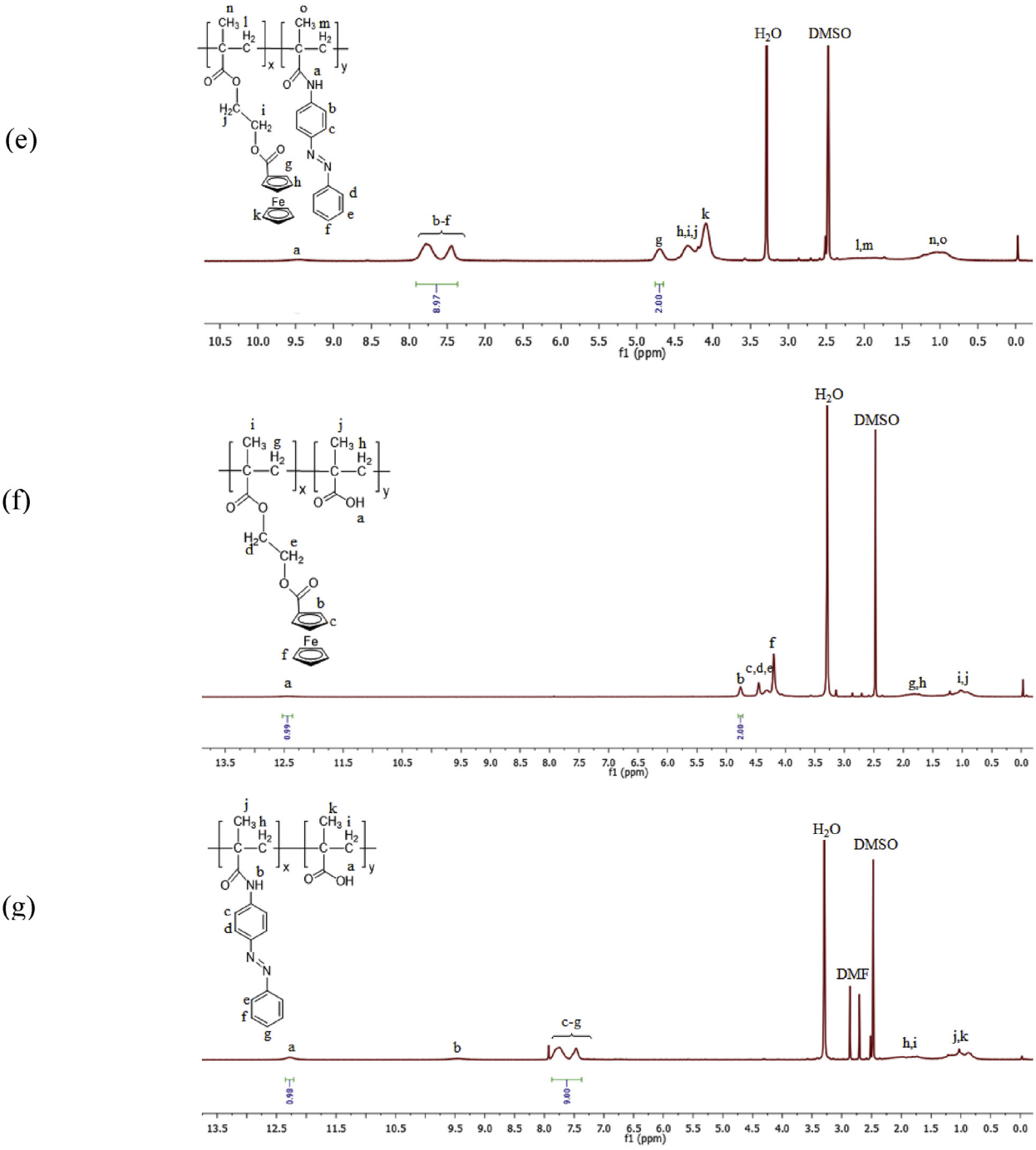

Fig. 1. (*continued*).

analysis (Fig. 3).

The chemical shifts for P(FHEMA-*co*-MAZO-*co*-MAA)-1 were as follows: δ (ppm) = 12.37 (H_a), 7.39–7.92 (H_b-H_f), 4.73 (H_g), 4.23–4.45 (H_h, H_i, H_j), 4.15 (H_k), 1.64–2.10 (H_l, H_m, H_n), 0.89–1.11 (H_o, H_p, H_q).

The chemical shifts for P(FHEMA-*co*-MAZO-*co*-MAA)-2 were as follows: δ (ppm) = 12.36 (H_a), 7.39–7.93 (H_b-H_f), 4.72 (H_g), 4.23–4.44 (H_h, H_i, H_j), 4.17 (H_k), 1.66–2.11 (H_l, H_m, H_n), 0.88–1.13 (H_o, H_p, H_q).

In FT-IR spectra (Fig. 3), the peaks at 3090-3097 cm^{-1} and 490-491 cm^{-1} belong to the stretching vibrations of ferrocene while the peak at 2925 cm^{-1} corresponds to the stretching vibration of aliphatic C–H [38–41]. The stretching vibration of N–H for amide group appeared at 3364-3368 cm^{-1} [42,43]. The stretching vibrations of C=O and benzene ring were observed at 1660-1661 cm^{-1} and 1520 cm^{-1} respectively [43,44].

Another important peak for N=N of azobenzene appeared at 1593-1595 cm^{-1} [45]. The stretching vibrations of C–O and bending vibrations of C–H were witnessed at 1160 cm^{-1} and 825-827 cm^{-1} respectively [40,42]. Table 3 comprised of the different band assignments for the functional groups. Fig. 4A shows the GPC curves of the different synthesized polymers. The copolymers showed PDI in the range of 1.49–1.90. TGA curves (Fig. 4B) indicated that the degradation of the respective polymers occurred in multiple stages. The initial decomposition of the copolymers

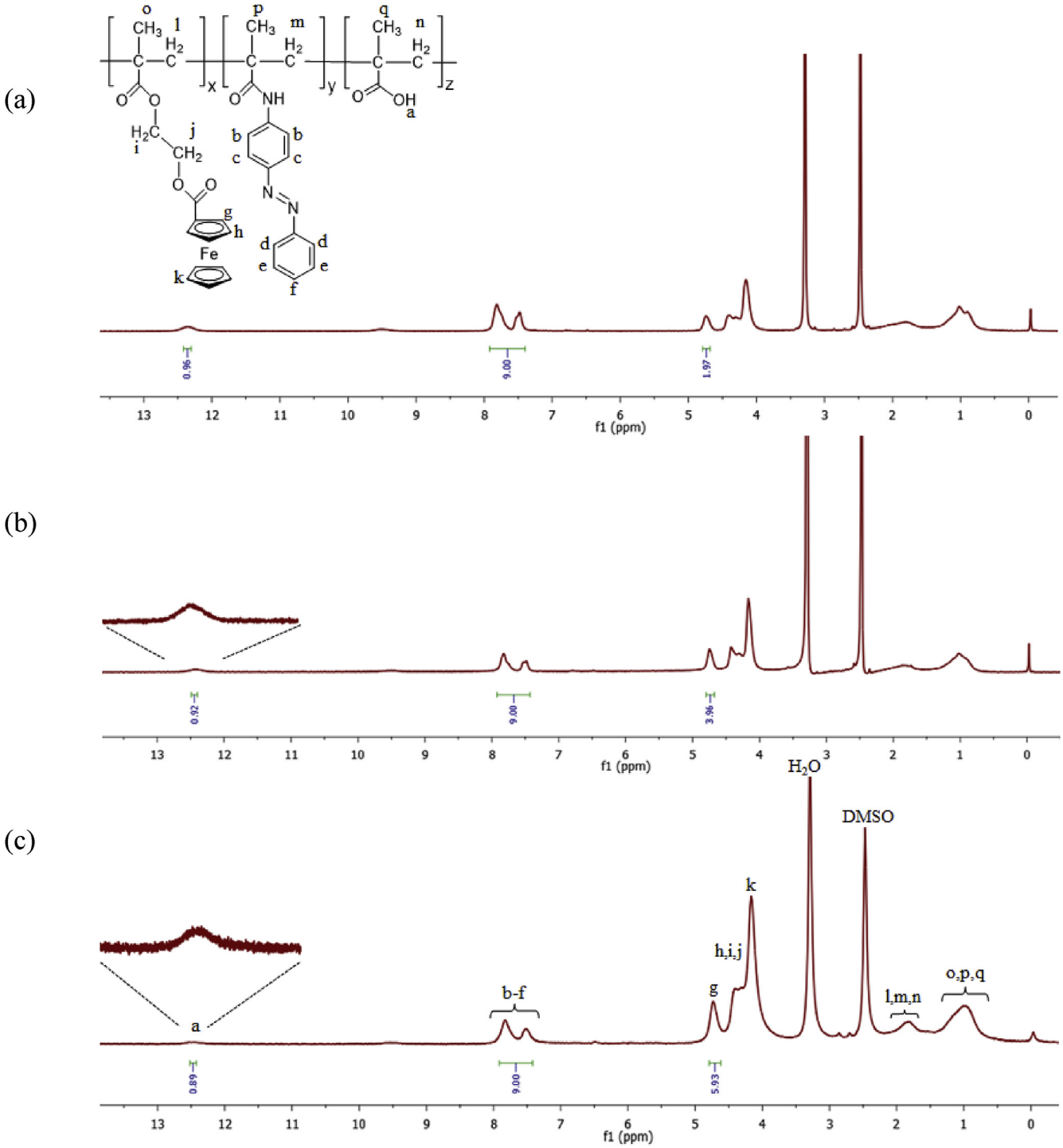

Fig. 2. ^{1}H NMR spectra of (a) P(FHEMA-*co*-MAZO-*co*-MAA)-1, (b) P(FHEMA-*co*-MAZO-*co*-MAA)-2 and (c) P(FHEMA-*co*-MAZO-*co*-MAA)-3.

ascribed to the breakage of azo groups [46]. This initial putrefaction of P(FHEMA-*co*-MAZO-*co*-MAA)-1, P(FHEMA-*co*-MAZO-*co*-MAA)-2 and P(FHEMA-*co*-MAZO-*co*-MAA)-3 appeared at 204 °C, 210 °C and 220 °C respectively. After that, the bonds (C═O and C—O) associated with the ferrocene were decomposed which generated a large extent of CO_2. This production of carbon dioxide is possibly responsible for the weight loss of the second stage [47].

The temperature at this stage appeared as 341 °C for P(FHEMA-*co*-MAZO-*co*-MAA)-1, 350 °C for P(FHEMA-*co*-MAZO-*co*-MAA)-2 and 358 °C for P(FHEMA-*co*-MAZO-*co*-MAA)-3. The thermal stability was increased due to the higher portion of ferrocene content. Finally, Fe—C bonds were broken down which formed enlarge amount of Fe atoms which expectedly catalyzed the degradation of the polymer after 525 °C.

The similar three different stages can be observed from the DTG curves (Fig. 4C). Fig. 4D represents the DSC curves of synthesized copolymers which revealed that T_g of the copolymers depends on the final percentage of ferrocene and azobenzene. P(FHEMA-*co*-

MAZO-*co*-MAA)-1, P(FHEMA-*co*-MAZO-*co*-MAA)-2 and P(FHEMA-*co*-MAZO-*co*-MAA)-3 depicted T_g of 152 °C, 145 °C and 130 °C respectively. The T_g value was gradually decreased from P(FHEMA-*co*-MAZO-*co*-MAA)-1 to P(FHEMA-*co*-MAZO-*co*-MAA)-3 in the obtained copolymers possibly due to the decrease in number average molecular weight (M_n) and azobenzene contents in the copolymer. This criteria was well explained by Carvalho and co-workers [48]. According to them, the M_n value and azo contents are directly related to the glass transition temperature of the polymers. In P(FHEMA-co-MAZO-co-MAA)-3, the obtained M_n value and azo contents were least which in turn reduced the size, rigidity and the polarity of the polymer chains.

3.2. Photo isomerization properties of P(FHEMA-co-MAZO-co-MAA)s

It is widely established that azo polymers show photo isomerization under different irradiations of UV and visible light. Mostly, the E → Z photoisomerization of azo polymers is predominant and driven by UV irradiations while visible light drove examples are very few [49–51]. *Trans* state of azobenzene brings an intense absorption peak while the *cis* state exhibits a weak absorption peak. The intense peak appears due to the π-π* transition whereas the weak absorption peak appears due to the n-π* transition [52]. These intense and weak absorptions bring reversible changes in the isomerization of azobenzene due to the light irradiations such as UV or visible. Heat can also take part in the reversible isomerization

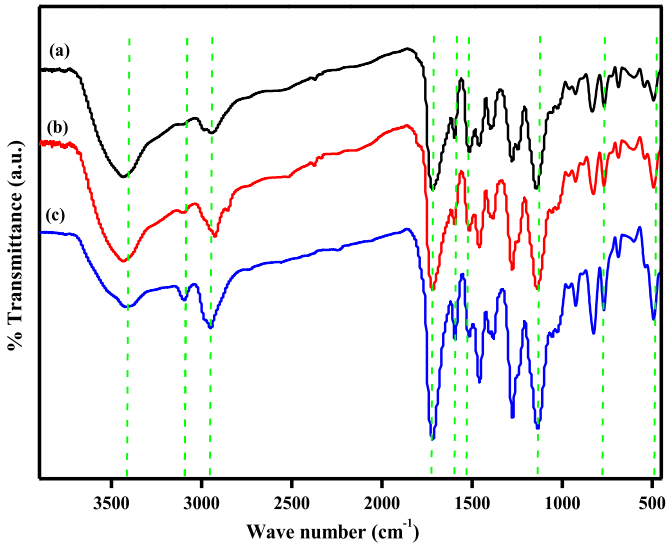

Fig. 3. FT-IR spectra of (a) P(FHEMA-*co*-MAZO-*co*-MAA)-1, (b) P(FHEMA-*co*-MAZO-*co*-MAA)-2 and (c) P(FHEMA-*co*-MAZO-*co*-MAA)-3.

which brings the *cis* state to its origin [53]. The thermal isomerization from *cis*-to-*trans* isomer proceeds because the activation energy of the *cis*-to-*trans* isomerization process is generally low. These isomerizations are generally followed by dramatic changes in some properties such as dipole moment and many others [51]. In this study, sample solutions of the synthesized copolymers were prepared in DMF, and the photoisomerizations of azo groups were investigated using UV–vis spectra. Fig. 5 explains the UV/vis spectra of the copolymers P(FHEMA-*co*-MAZO-*co*-MAA)s obtained after the UV irradiation (365 nm) and visible irradiation. In Fig. 5, the spectrum of the non-irradiated sample showed two absorption bands; the first absorption band was of *trans* isomer of azobenzene which appeared at 356 nm (π-π* transition) while the second band appeared at 440 nm due to n-π* transition (*cis* isomer). The band at 356 nm was changed noticeably upon UV irradiation owing to the π-π* electronic excitation [29,54]. The subsequent irradiation of UV light for 300 s converted the *trans* isomers into *cis* forms. It can also be noticed from Fig. 5(a–c) that by increasing the time of UV irradiation, the absorption band at 440 nm started to increase slightly. However, due to the small absorptivity of the n-π* transition, this band cannot be adopted for quantitative analysis [55].

Another important spectra were recorded for the *cis* to *trans* isomerization using visible light as shown in Fig. 5 (a'-c'). The first spectrum was recorded after UV irradiation for 5 min to make sure the conversion of *trans* isomers to the other isomeric form (*cis*). This irradiation showed two absorption bands, the first band appeared at 356 nm while the other band at 440 nm. After that, the visible light was irradiated on the same sample solution for 2 min which helped the *cis* isomers converting back to the *trans* form. Due to visible light irradiation, the peak at 356 nm has started to increase. This corresponds that the *cis* isomers have started to convert to their more stable *trans* form. Subsequent irradiation of visible light showed a gradual increase in peak intensity at 356 nm. Complete recovery of the *trans* isomers has achieved gradually by increasing the time of visible light irradiation. This *trans*-to-*cis* and *cis*-to-*trans* isomerization of the copolymers evidenced that the copolymers have reversible photo isomerization behavior. The information storage behavior was improved in comparison with our previously reported work without MAA [34]. As it can be observed from Fig. 5 (a'-c') that the copolymers returned to their initial state after 15 min of visible irradiation. This effect was not obtained in the previously reported copolymers without MAA [34].

3.3. Electrochemical properties of P(FHEMA-co-MAZO-co-MAA)s

The electrochemical properties are very essential to investigate the redox-responsive nature of the ferrocene-based copolymers. In principle, the electrochemical process contains loss and gain of electrons. There are many methods available which can determine the electrochemical nature. Among the available methods, CV is

Table 3
FT-IR data of P(FHEMA-*co*-MAZO-*co*-MAA)-1, P(FHEMA-*co*-MAZO-*co*-MAA)-2 and P(FHEMA-*co*-MAZO-*co*-MAA)-3.

P (FHEMA-*co*-MAZO-*co*-MAA)s			Band assignment [38–45]
P (FHEMA-co-MAZO-co-MAA)-1	P (FHEMA-co-MAZO-co-MAA)-2	P (FHEMA-co-MAZO-co-MAA)-3	
3364	3368	3368	N–H str.
3090	3095	3097	C–H str. of Cp rings
2925	2925	2925	Aliphatic C–H str.
1660	1661	1660	C=O str.
1520	1520	1520	Benzene ring str.
1595	1595	1593	N=N str.
1160	1160	1160	C–O str.
825	827	827	C–H bend.
491	490	490	Cp-Fe str.

considered as one of the most accurate and reliable methods for the determination of electrochemical properties. Thereby, the electrochemical properties of the synthesized copolymers (P(FHEMA-*co*-MAZO-*co*-MAA)s) were evaluated by CV [56].

It is well known that different parameters such as the concentration of supporting electrolyte, potential scan rates and solvent polarity etc. can affect the charge properties of the polymers [57–61]. Therefore, the copolymers solution (0.5 mM) were prepared using a supporting electrolyte *i.e.* Bu_4NBF_4 (0.1 M) in different organic solvents (DCM, DMSO, DMF, THF). The selection of these solvents was done on the basis of their polarity difference. The peaks were found deformed and compact by increasing the polarity and viscosity of the solvents. For instance, the CV curves were found more deformed in DMSO or DMF as compared to the DCM. On the other hand, due to the compact nature of the peaks, it can also be concluded that the oxidized state of ferrocene was stable enough and difficult to reduce in highly polar solvents, which in turn showed more than one redox peak in the case of DMF and DMSO especially. In DCM, the electrode reactions were faster which provided one distinct reduction and oxidation peak in the results. The polarity of the solvents showed a direct relationship with the reduction and oxidation process of the copolymers which can also be observed from the results, as the peak potential of oxidation and reduction process was getting decrease with increasing solvent polarity [62].

Peaks were sharp and well defined whereas the lowest peak-to-peak potential separation (ΔEp) was also observed in DCM. All these results showed that electrochemical reactions were more favorable in DCM in comparison with the other solvents Figs. 6–8. For a better understanding of redox/photoresponsive based multi-states information storage, a schematic view has been shown in Fig. 9. In the first step, UV light incidents and *trans* azobenzene changes to *cis* azobenzene which can be regarded as state 2 ((a) storage of optical information). In the third state, electrical information is stored, when ferrocene changes to ferrocenium ion ((b) storage of electrical information). The fourth state corresponds with *cis* to *trans* isomerization of azobenzene after consuming the visible light ((c) storage of optical information) and lastly ferrocenium ion turns into its initial state after retrieving the electrical information ((d) storage of electrical information).

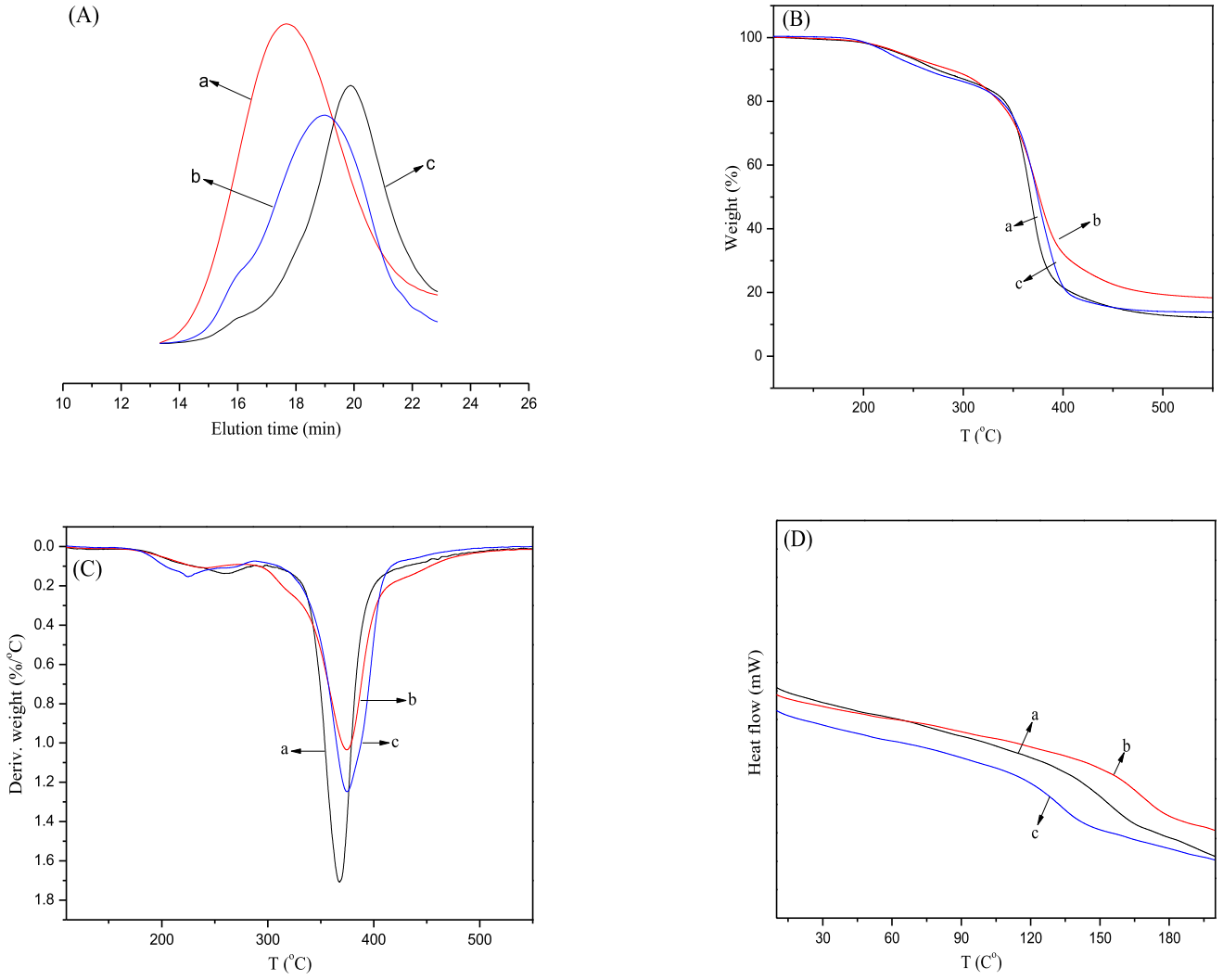

Fig. 4. (A) GPC curves of (a) P(FHEMA-*co*-MAZO-*co*-MAA)-1, (b) P(FHEMA-*co*-MAZO-*co*-MAA)-2 and (c) P(FHEMA-*co*-MAZO-*co*-MAA)-3; (B) TGA curves of (a) P(FHEMA-*co*-MAZO-*co*-MAA)-1, (b) P(FHEMA-*co*-MAZO-*co*-MAA)-2 and (c) P(FHEMA-*co*-MAZO-*co*-MAA)-3; (C) DTG curves of (a) P(FHEMA-*co*-MAZO-*co*-MAA)-1, (b) P(FHEMA-*co*-MAZO-*co*-MAA)-2 and (c) P(FHEMA-*co*-MAZO-*co*-MAA)-3 and (D) DSC curves of (a) P(FHEMA-*co*-MAZO-*co*-MAA)-1, (b) P(FHEMA-*co*-MAZO-*co*-MAA)-2 and (c) P(FHEMA-*co*-MAZO-*co*-MAA)-3.

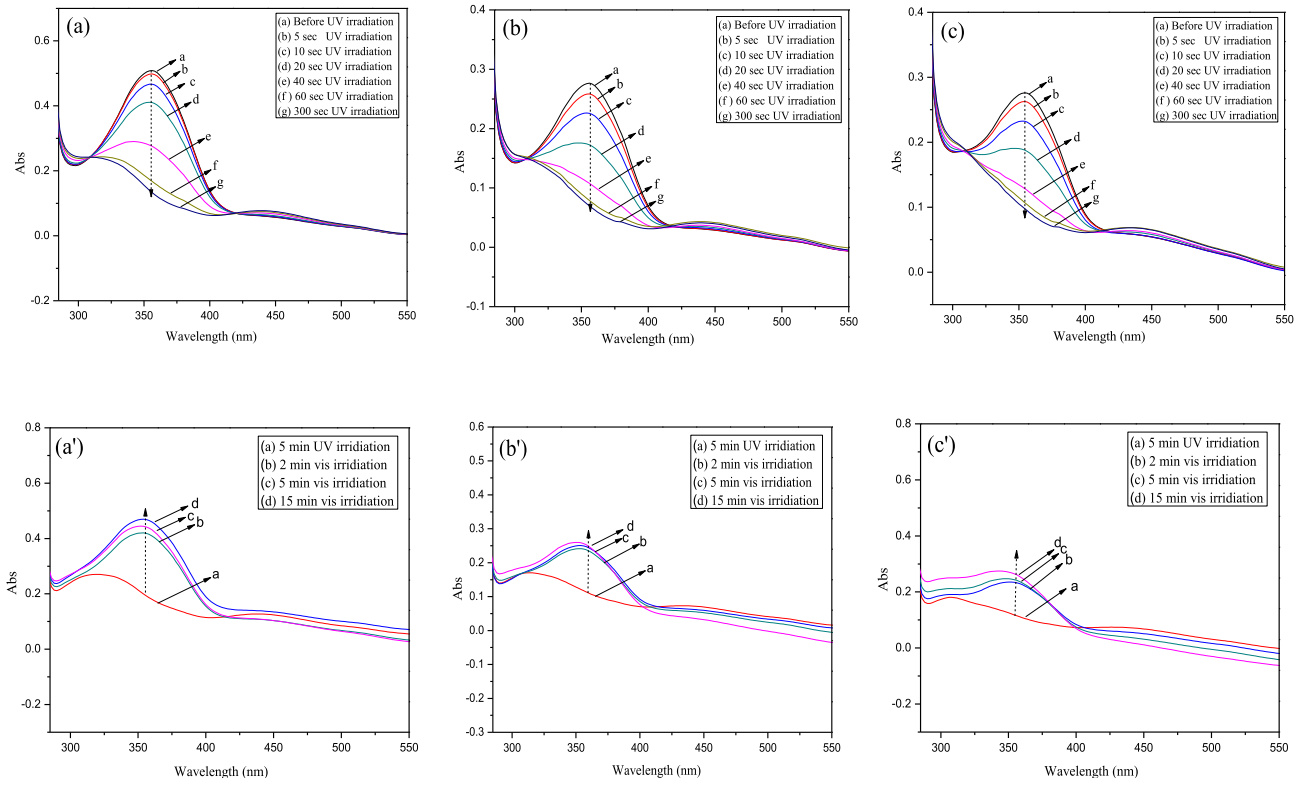

Fig. 5. UV/vis spectra of (a) P(FHEMA-*co*-MAZO-*co*-MAA)-1, (b) P(FHEMA-*co*-MAZO-*co*-MAA)-2 and (c) P(FHEMA-*co*-MAZO-*co*-MAA)-3 at different time intervals of UV light; UV/vis spectra of (a') P(FHEMA-*co*-MAZO-*co*-MAA)-1, (b') P(FHEMA-*co*-MAZO-*co*-MAA)-2 and (c') P(FHEMA-*co*-MAZO-*co*-MAA)-3 at different time intervals of UV and visible light irradiation.

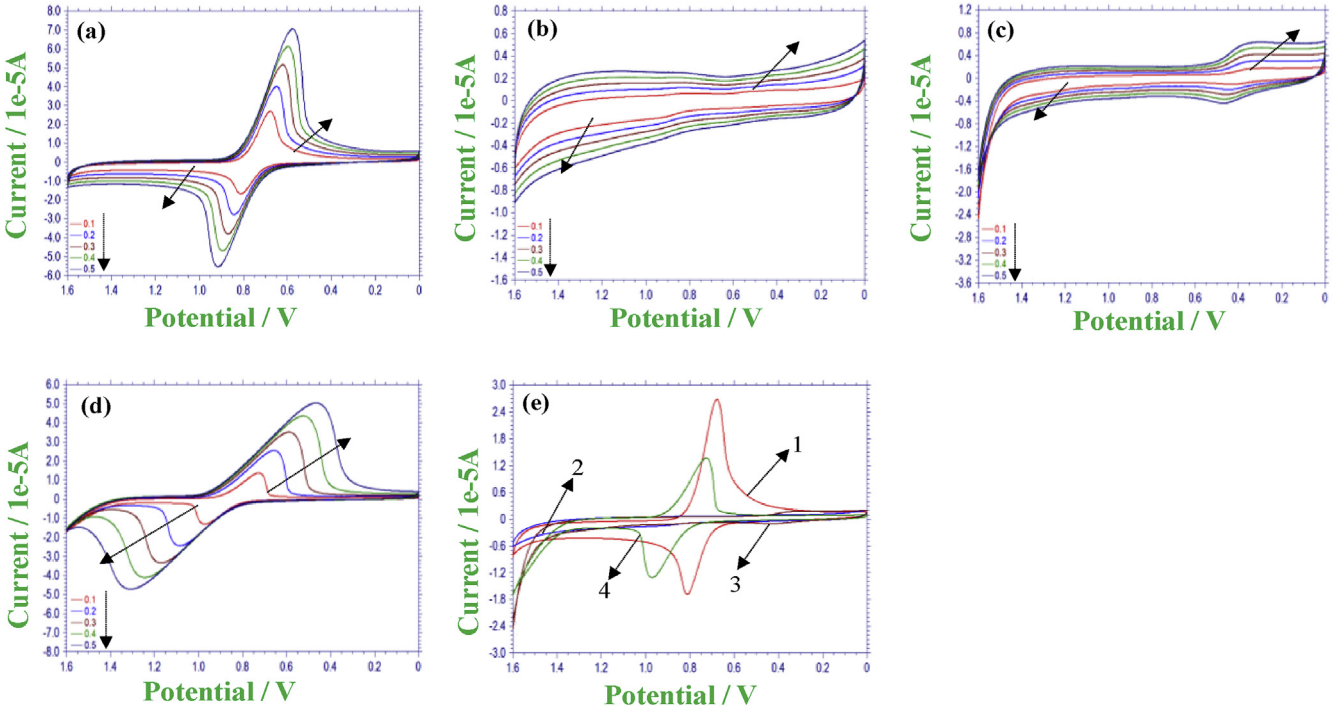

Fig. 6. CV curves of P(FHEMA-*co*-MAZO-*co*-MAA)-1 in (a) DCM, (b) DMF, (c) DMSO and (d) THF at different potential scan rates (direction of arrows means the increase of peaks in terms of current (oxidation and reduction) by increasing the scan rate) and (e) different organic solvents: (1) DCM, (2) DMF, (3) DMSO and (4) THF at 0.1 V/s.

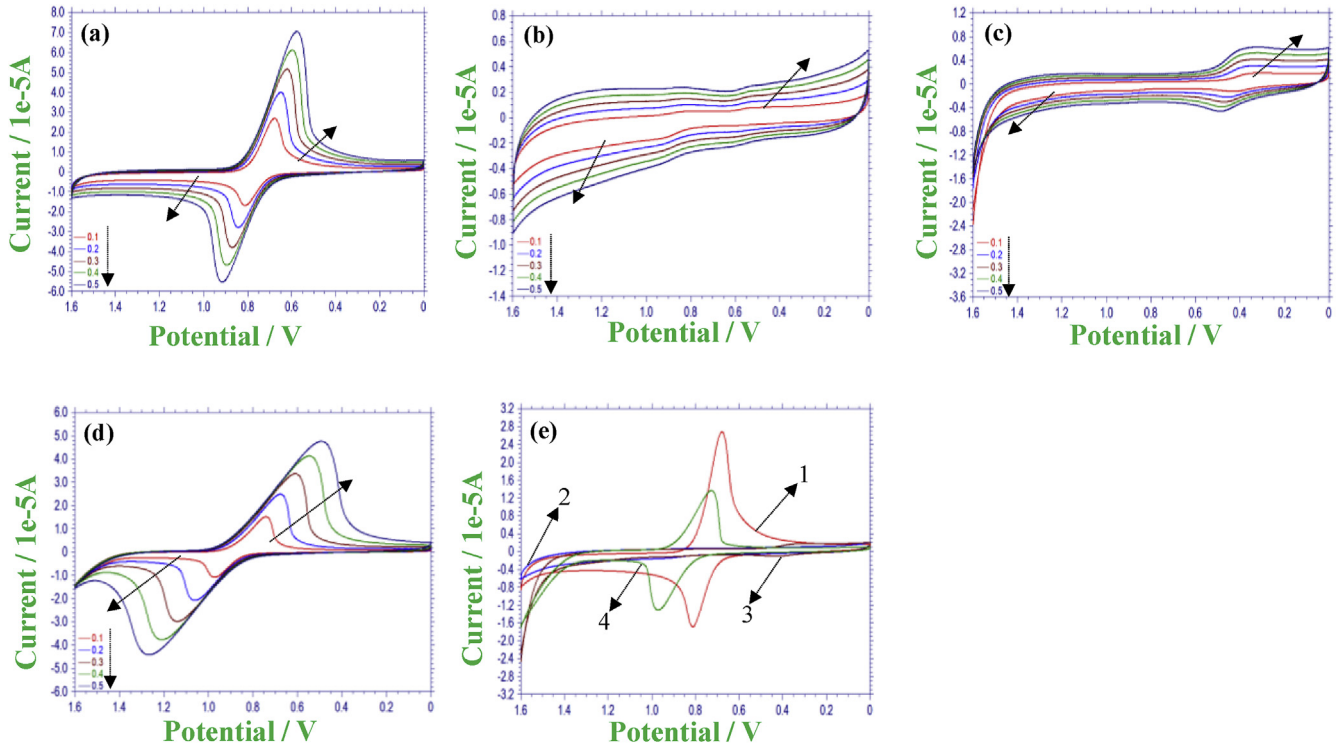

Fig. 7. CV curves of P(FHEMA-*co*-MAZO-*co*-MAA)-2 in (a) DCM, (b) DMF, (c) DMSO and (d) THF at different potential scan rates (direction of arrows means the increase of peaks in terms of current (oxidation and reduction) by increasing the scan rate) and (e) different organic solvents: (1) DCM, (2) DMF, (3) DMSO and (4) THF at 0.1 V/s.

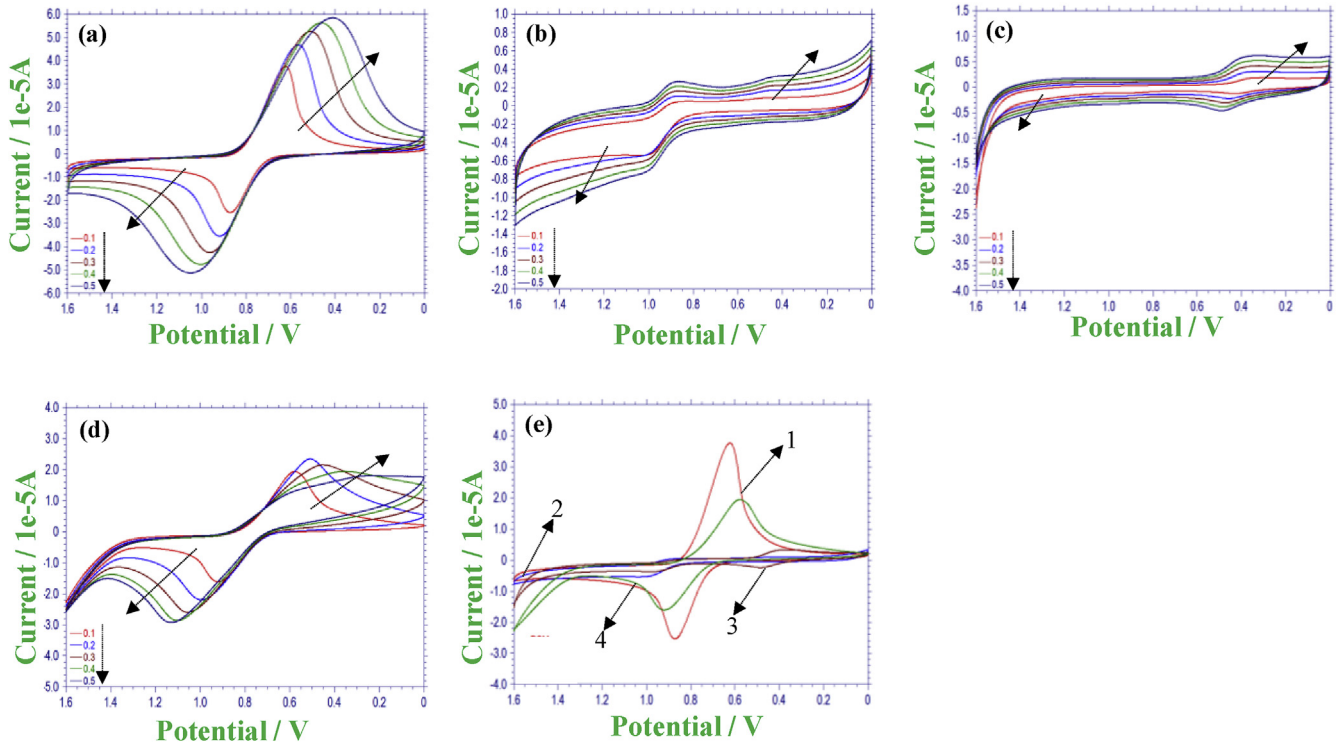

Fig. 8. CV curves of P(FHEMA-*co*-MAZO-*co*-MAA)-3 in (a) DCM, (b) DMF, (c) DMSO and (d) THF at different potential scan rates (direction of arrows means the increase of peaks in terms of current (oxidation and reduction) by increasing the scan rate) and (e) different organic solvents: (1) DCM, (2) DMF, (3) DMSO and (4) THF at 0.1 V/s.

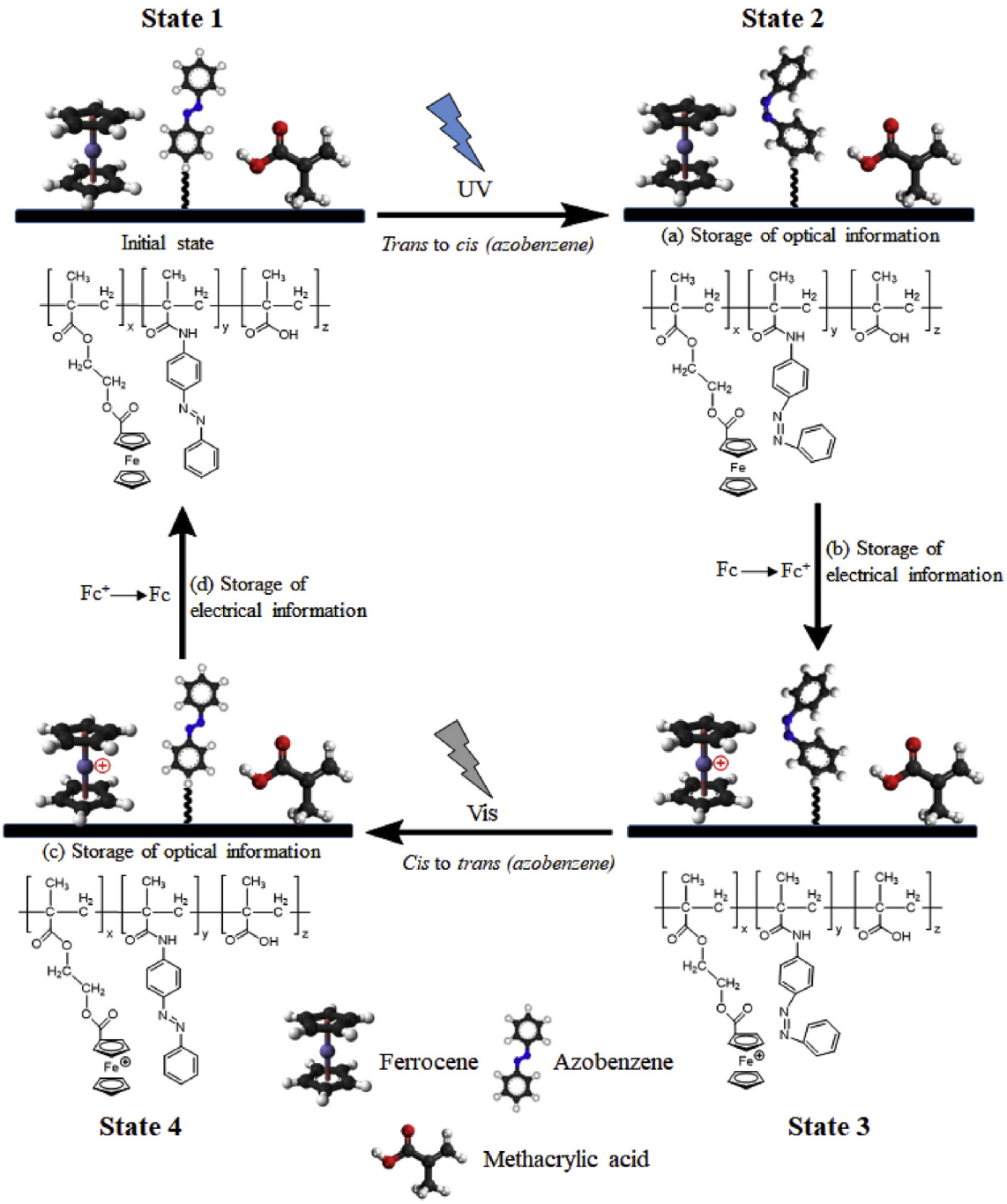

Fig. 9. Schematic model of the multi-state information storage.

4. Conclusion

In the present work, (P(FHEMA-*co*-MAZO-*co*-MAA)s) were synthesized and their information storage behavior was analyzed. The enhancement of photostability in azobenzene chromophores is an important system for the information storage device. Therefore, methacrylic acid was introduced as a side group to affect the properties [35]. The synthesized copolymers were characterized by ^{1}H NMR spectra and GPC results. Thermal analysis was performed by TG/DTG and DSC techniques. Redox studies and photo responsive studies were performed by CV technique and UV/vis spectroscopy which showed that these copolymers had good redox and photo responsive properties.

The polymers were found sustained to different intervals of UV–vis light irradiation while the polymers showed reversible *trans*/*cis* switching after a certain interval of visible light. The obtained results paved the way towards the four states information storage of the materials. All these characteristics showed that these polymers can provide valuable redox/photo responsive performance which can be further applied for the storage of information.

Acknowledgment

Financial support from the National Natural Science Foundation

of China (51673170, 21472168, 21372200 and 21611530689), the Fundamental Research Funds for the Central Universities (2017FZA4023) are gratefully acknowledged.

References

[1] Q.D. Ling, D.J. Liaw, Y.H. Teo, C. Zhu, S.H. Chan, E.T. Kang, K.G. Neoh, Polymer 48 (2007) 5182–5201.
[2] Q.D. Ling, D.J. Liaw, C. Zhu, S.H. Chan, E.T. Kang, K.G. Neoh, Prog. Polym. Sci. 33 (2008) 917–978.
[3] Y. Chen, G. Liu, C. Wang, W. Zhang, R.W. Li, L. Wang, Mater. Horiz. 1 (2014) 489–506.
[4] T. Kurosawa, T. Higashihara, M. Ueda, Polym. Chem. 4 (2013) 16–30.
[5] A. Pecora, L. Maiolo, M. Cuscunà, D. Simeone, A. Minotti, L. Mariucci, G. Fortunato, Solid State Electron. 52 (2008) 348–352.
[6] M. Kondo, M. Sugimoto, M. Yamada, Y. Naka, J.I. Mamiya, M. Kinoshita, A. Shishido, Y. Yu, T. Ikeda, J. Mater. Chem. 20 (2009) 117–122.
[7] K.M. Roth, N. Dontha, R.B. Dabke, D.T. Gryko, C. Clausen, J.S. Lindsey, D.F. Bocian, W.G. Kuhr, J. Vac. Sci. Technol. B 18 (2000) 2359–2364.
[8] S. Wang, F. Li, A.D. Easley, J.L. Lutkenhaus, Nat. Mater. 18 (2019) 69–75.
[9] T. Yamamoto, T. Morikita, T. Maruyama, K. Kubota, M. Katada, Macromolecules 30 (1997) 5390–5396.
[10] Y.V. Zatsikha, C.D. Holstrom, K. Chanawanno, A.J. Osinski, C.J. Ziegler, V.N. Nemykin, Inorg. Chem. 56 (2017) 991–1000.
[11] A. Vecchi, N.R. Erickson, J.R. Sabin, B. Floris, V. Conte, M. Venanzi, P. Galloni, V.N. Nemykin, Chem. Eur J. 21 (2015) 269–279.
[12] T.J. Kealy, P.L. Pauson, Nature 168 (1951) 1039–1040.
[13] J. Rochford, A.D. Rooney, M.T. Pryce, Inorg. Chem. 46 (2007) 7247–7249.
[14] E. Maligaspe, M.R. Hauwiller, Y.V. Zatsikha, J.A. Hinke, P.V. Solntsev, D.A. Blank, V.N. Nemykin, Inorg. Chem. 53 (2014) 9336–9347.
[15] H. Tan, H. Yao, Y. Song, S. Zhu, H. Yu, S. Guan, Dyes Pigments 146 (2017) 210–218.
[16] C. Jin, J. Lee, E. Lee, E. Hwang, H. Lee, Chem. Commun. 48 (2012) 4235–4237.
[17] F.A. Larik, A. Saeed, T.A. Fattah, U. Muqadar, P.A. Channar, Appl. Organomet. Chem. 31 (2017) 1–19.
[18] Q. Li, G. Mathur, M. Homsi, S. Surthi, V. Misra, V. Malinovskii, K.-H. Schweikart, L. Yu, J.S. Lindsey, Z. Liu, Appl. Phys. Lett. 81 (2002) 1494–1496.
[19] Q. Li, G. Mathur, S. Gowda, S. Surthi, Q. Zhao, L. Yu, J.S. Lindsey, D.F. Bocian, V. Misra, Adv. Mater. 16 (2004) 133–137.
[20] Z.F. Liu, K. Hashimoto, A. Fujishima, Nature 347 (1990) 658–665.
[21] A. Natansohn, P. Rochon, Chem. Rev. 102 (2002) 4139–4176.
[22] T. Ikeda, O. Tsutsumi, Science 268 (1995) 1873–1875.
[23] T. Hugel, N.B. Holland, A. Cattani, L. Moroder, M. Seitz, H.E. Gaub, Science 296 (2002) 1103–1106.
[24] Y. Munenori, K. Mizuho, M. Jun-Ichi, Y. Yanlei, K. Motoi, C.J. Barrett, I. Tomiki, Angew. Chem. Int. Ed. 47 (2010), 4940-4940.
[25] J. Isayama, S. Nagano, T. Seki, Macromolecules 43 (2010) 4105–4112.
[26] Y. Bai, J. Hu, W. Shen, X. Hu, Polym. Int. 63 (2014) 1539–1544.
[27] B.K. Pathem, Y.B. Zheng, J.L. Payton, T.-B. Song, B.-C. Yu, J.M. Tour, Y. Yang, L. Jensen, P.S. Weiss, J. Phys. Chem. Lett. 3 (2012) 2388–2394.
[28] A. Emoto, E. Uchida, T. Fukuda, Polymers 4 (2012) 150–186.
[29] H.D. Bandara, S.C. Burdette, Chem. Soc. Rev. 41 (2012) 1809–1825.
[30] M. Moniruzzaman, P. Zioupos, G. Fernando, Scr. Mater. 54 (2006) 257–261.
[31] A. Richter, M. Nowicki, B. Wolf, Mol. Cryst. Liq. Cryst. 483 (2008) 49–61.
[32] S.L. Lim, N.-J. Li, J.-M. Lu, Q.-D. Ling, C.X. Zhu, E.-T. Kang, K.G. Neoh, ACS Appl. Mater. Interfaces 1 (2008) 60–71.
[33] B. Zhang, L. Liu, L. Wang, B. Liu, X. Tian, Y. Chen, Carbon 134 (2018) 500–506.
[34] A. Khan, L. Wang, H. Yu, M. Haroon, R.S. Ullah, A. Nazir, T. Elshaarani, M. Usman, S. Fahad, K.-u.-R. Naveed, J. Organomet. Chem. 880 (2018) 124–133.
[35] A. Galvan-Gonzalez, K. Belfield, G. Stegeman, M. Canva, K.-P. Chan, K. Park, L. Sukhomlinova, R. Twieg, Appl. Phys. Lett. 77 (2000) 2083–2085.
[36] M. Saleem, L. Wang, H. Yu, Zain-ul-Abdin, M. Akram, R.S. Ullah, Colloid Polym. Sci. 295 (2018) 995–1006.
[37] P. Weis, D. Wang, S. Wu, Macromolecules 49 (2016) 6368–6373.
[38] W. He, F. Deng, Y.Y. Jiang, D. Wu, H. Fan, X. Jian, Chin. Chem. Lett. 21 (2010) 748–752.
[39] Z.U. Abdin, W. Li, H. Yu, M. Saleem, M. Akram, N.M. Abbasi, H. Khalid, R. Sun, Y. Chen, New J. Chem. 40 (2016) 3155–3163.
[40] S. Mehdipour-Ataei, S. Babanzadeh, Appl. Organomet. Chem. 21 (2010) 360–367.
[41] M. Cazacu, A. Vlad, M. Marcu, C. Racles, A. Airinei, G. Munteanu, Macromolecules 39 (2006) 3786–3793.
[42] A. Nigar, M.S.U. Khan, Z. Akhter, M.S. Butt, Some new organometallic polyamides based on ferrocene, J. Inorg. Organomet. Polym. Mater. 17 (2007) 509–516.
[43] Z. Akhter, M.A. Bashir, M.S.U. Khan, Appl. Organomet. Chem. 19 (2010) 848–853.
[44] X. Xia, H. Yu, L. Wang, Z. Deng, K.J. Shea, Zain-ul-Abdin, Eur. Polym. J. 100 (2018) 103–110.
[45] Z. Akhter, M.S.U. Khan, M.A. Bashir, J. Inorg. Organomet. Polym. 14 (2004) 253–267.
[46] A.S. Abd-El-Aziz, T.H. Afifi, W.R. Budakowski, K.J. Friesen, E.K. Todd, Macromolecules 35 (2002) 8929–8932.
[47] W.A. Amer, W. Li, A.M. Amin, H. Yu, Z. Lei, L. Chao, W. Yang, Polym. Adv. Technol. 24 (2013) 181–190.
[48] L.L. Carvalho, T.F.C. Borges, M.R. Cardoso, C.R. Mendonça, D.T. Balogh, Eur. Polym. J. 42 (10) (2006) 2589–2595.
[49] W. Zhang, K. Yoshida, M. Fujiki, X. Zhu, Macromolecules 44 (2011) 5105–5111.
[50] L. Wang, X. Pan, Y. Zhao, Y. Chen, W. Zhang, Y. Tu, Z. Zhang, J. Zhu, N. Zhou, X. Zhu, Macromolecules 48 (2015) 1289–1295.
[51] A. Izumi, M. Teraguchi, R. Nomura, T. Masuda, Macromolecules 33 (2000) 5347–5352.
[52] G. Zimmerman, L.-Y. Chow, U.-J. Paik, J. Am. Chem. Soc. 80 (1958) 3528–3531.
[53] G.S. Kumar, D. Neckers, Chem. Rev. 89 (1989) 1915–1925.
[54] P. Christogianni, M. Moniruzzaman, G. Kister, Polymer 77 (2015) 272–277.
[55] Y. Shuai, D. Yusheng, W. Weifeng, H. Yun, Z. Jianshe, J. Phys. Chem. A 112 (2008) 13326–13334.
[56] N.G. Tsierkezos, J. Solut. Chem. 36 (2007) 289–302.
[57] L. Ma, L. Wang, Q. Tan, H. Yu, J. Huo, Z. Ma, H. Hu, Z. Chen, Electrochim. Acta 54 (2009) 5413–5420.
[58] Q. Tan, L. Wang, L. Ma, H. Yu, Q. Liu, A. Xiao, Macromolecules 42 (2009) 4500–4510.
[59] C. Li, L. Wang, L. Deng, H. Yu, J. Huo, L. Ma, J. Wang, J. Phys. Chem. B 113 (2009) 15141–15144.
[60] H. Yu, L. Wang, J. Huo, C. Li, Q. Tan, Des. Monomers Polym. 12 (2009) 305–313.
[61] T. Chen, L. Wang, G. Jiang, J. Wang, X. Jie Wang, J. Zhou, J. Wang, C. Chen, W. Wang, H. Gao, J. Electroanal. Chem. 586 (2006) 122–127.
[62] A.J. Bard, L.R. Faulkner, Russ. J. Electrochem. 38 (2002) 1364–1365.